HHS Public Access

Author manuscript

Mol Pharm. Author manuscript; available in PMC 2024 July 16.

Published in final edited form as:

Mol Pharm. 2024 June 03; 21(6): 2727–2739. doi:10.1021/acs.molpharmaceut.3c01105.

In Vivo Delivery of Spherical and Cylindrical *In Vitro* Reconstituted Virus-like Particles Containing the Same Self-Amplifying mRNA

Sweta Karan[#],
Department of NanoEngineering, Center for Nano-ImmunoEngineering, and Shu and K. C. Chien and Peter Farrell Collaboratory, University of California San Diego, La Jolla, California 92093, United States

Ana Luisa Durán-Meza[#],
Department of Chemistry and Biochemistry, University of California, Los Angeles, California 90095, United States

Abigail Chapman,
Department of Chemistry and Biochemistry, University of California, Los Angeles, California 90095, United States

Cheylene Tanimoto,
Department of Chemistry and Biochemistry, University of California, Los Angeles, California 90095, United States; California NanoSystems Institute, University of California, Los Angeles, California 90095, United States

Soo Khim Chan,
Department of NanoEngineering and Center for Nano-ImmunoEngineering, University of California San Diego, La Jolla, California 92093, United States

Charles M. Knobler,
Department of Chemistry and Biochemistry, University of California, Los Angeles, California 90095, United States;

William M. Gelbart,

Corresponding Authors: **William M. Gelbart** – Department of Chemistry and Biochemistry, University of California, Los Angeles, California 90095, United States; UCLA Molecular Biology Institute and California NanoSystems Institute, University of California, Los Angeles, California 90095, United States; gelbart@chem.ucla.edu, **Nicole F. Steinmetz** – Department of NanoEngineering, Center for Nano-ImmunoEngineering, Institute for Materials Discovery and Design, Department of Bioengineering, Department of Radiology, Moores Cancer Center, and Shu and K. C. Chien and Peter Farrell Collaboratory, University of California San Diego, La Jolla, California 92093, United States; Center for Engineering in Cancer, Institute for Engineering in Medicine, University of California, San Diego, La Jolla, California 92093, United States; nsteinmetz@ucsd.edu.

[#]Author Contributions

S.K. and A.L.D.-M. contributed equally to this work.

Supporting Information

The Supporting Information is available free of charge at https://pubs.acs.org/doi/10.1021/acs.molpharmaceut.3c01105.
Cloning strategy; additional analysis of *in vitro* transcribed mRNA analyzed; additional TEM of VLPs and proteins; additional characterization of expression of mRNA cassettes; characterization of fluorescent VLPs; and additional IVIS imaging data (PDF)

Complete contact information is available at: https://pubs.acs.org/10.1021/acs.molpharmaceut.3c01105

The authors declare the following competing financial interest(s): N.F.S. is a co-founder of, has equity in, and has a financial interest in Mosaic ImmunoEnginering Inc. and is a co-founder and serves as manager of Pokometz Scientific LLC, under which she is a paid consultant to Mosaic ImmunoEngineering Inc., Flagship Labs 95 Inc., and Arana Biosciences Inc.

Department of Chemistry and Biochemistry, University of California, Los Angeles, California 90095, United States; UCLA Molecular Biology Institute and California NanoSystems Institute, University of California, Los Angeles, California 90095, United States;

Nicole F. Steinmetz
Department of NanoEngineering, Center for Nano-ImmunoEngineering, Institute for Materials Discovery and Design, Department of Bioengineering, Department of Radiology, Moores Cancer Center, and Shu and K. C. Chien and Peter Farrell Collaboratory, University of California San Diego, La Jolla, California 92093, United States; Center for Engineering in Cancer, Institute for Engineering in Medicine, University of California, San Diego, La Jolla, California 92093, United States;

Abstract

The dramatic effectiveness of recent mRNA (mRNA)-based COVID vaccines delivered in lipid nanoparticles has highlighted the promise of mRNA therapeutics in general. In this report, we extend our earlier work on self-amplifying mRNAs delivered in spherical *in vitro* reconstituted virus-like particles (VLPs), and on drug delivery using cylindrical virus particles. In particular, we carry out separate *in vitro* assemblies of a self-amplifying mRNA gene in two different virus-like particles: one spherical, formed with the capsid protein of cowpea chlorotic mottle virus (CCMV), and the other cylindrical, formed from the capsid protein of tobacco mosaic virus (TMV). The mRNA gene is rendered self-amplifying by genetically fusing it to the RNA-dependent RNA polymerase (RdRp) of Nodamura virus, and the relative efficacies of cell uptake and downstream protein expression resulting from their CCMV- and TMV-packaged forms are compared directly. This comparison is carried out by their transfections into cells in culture: expressions of two self-amplifying genes, enhanced yellow fluorescent protein (EYFP) and Renilla luciferase (Luc), packaged alternately in CCMV and TMV VLPs, are quantified by fluorescence and chemiluminescence levels, respectively, and relative numbers of the delivered mRNAs are measured by quantitative real-time PCR. The cellular uptake of both forms of these VLPs is further confirmed by confocal microscopy of transfected cells. Finally, VLP-mediated delivery of the self-amplifying-mRNA in mice following footpad injection is shown by *in vivo* fluorescence imaging to result in robust expression of EYFP in the draining lymph nodes, suggesting the potential of these plant virus-like particles as a promising mRNA gene and vaccine delivery modality. These results establish that both CCMV and TMV VLPs can deliver their *in vitro* packaged mRNA genes to immune cells and that their self-amplifying forms significantly enhance *in situ* expression. Choice of one VLP (CCMV or TMV) over the other will depend on which geometry of nucleocapsid is self-assembled more efficiently for a given length and sequence of RNA, and suggests that these plant VLP gene delivery systems will prove useful in a wide variety of medical applications, both preventive and therapeutic.

Graphical Abstract

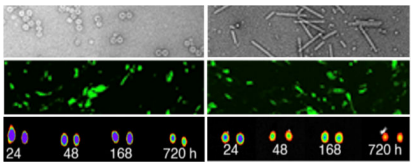

Keywords

self-amplifying mRNA; Nodamura replicon; tobacco mosaic virus (TMV); cowpea chlorotic mottle virus (CCMV); plant virus-like particles (VLPs); mRNA vaccine

INTRODUCTION

The COVID-19 pandemic highlights the opportunity and utility of platform nanotechnology for modern vaccine development.[1] The plug-and-play nature of mRNA vaccines in particular holds promise not just for readiness for emergent infectious diseases,[2] but also more generally to make an impact on human health in areas of chronic disease such as cancer, and cardiovascular, and neurodegenerative diseases.[3] Nanoparticle technologies are exploited to overcome the inherent instability of the active ingredient, the mRNA—and enable its targeting and uptake by immune cells. To further stabilize the labile mRNA, two key strategies are used: (1) chemical modifications of nucleotides, as well as capping and polyadenylation at the 5′ and 3′ends, respectively, make the nucleic acid less prone to hydrolysis and enzymatic degradation[4] and (2) self-amplifying mRNA (samRNA) replicons are used[5] in which the molecule remains unchanged, but its potency is boosted by strong replication within the target cell, resulting in enhanced protein expression even at lower doses.[5–7] Replicons exploit the molecular functions of viral replicases by fusing the replicase gene to a gene of interest, separated by a self-cleaving peptide sequence so that the gene is replicated along with the replicase gene, but their protein products are independent and functional. The field has grown out of its infancy and several samRNA-based vaccines have earned approval for clinical trials in humans against influenza, respiratory syncytial, rabies, Ebola, human papilloma, and human immunodeficiency viral infections.[8]

The replicons from mammalian alphaviruses such as Sindbis virus, Venezuelan equine encephalitis virus, and Semliki Forest virus (SFV) have been broadly explored as expression vectors, for gene therapy and for human vaccines.[9] These replicons are widely explored but have technical challenges: the insert is generally large (~9–15 kb), which can lead to genetic instability and limit nanoparticle encapsulation efficiencies. Furthermore, the larger inserts can trigger “danger signals” and lead to cytotoxicity due to the formation of dsRNA.[10,11] The Nodamura virus replicon has emerged as an alternative with positive attributes: it can replicate in diverse hosts including plant, yeast, and mammalian cells and, most importantly, it is one of the shortest known replicons with a length of only 3.2 knt.[7]

Synthetic carriers have made headway for clinical delivery of mRNA vaccines, e.g., both Moderna’s and Pfizer BioNTech’s COVID-19 vaccine technologies feature lipid nanoparticles.[12] Nevertheless, there is an opportunity to develop biomanufacturing approaches where biological building blocks are propagated and manufactured using self-replicating processes. This can overcome supply chain shortages, e.g., a lack of critical raw materials, such as chemical components required for synthetic carriers, which may be circumvented by having the mRNA vaccines produced through engineered living materials (ELMs). Specifically, our long-term vision is to produce the carrier and mRNA vaccine in a biological system, e.g., a plant could be used as the host for biomanufacture.[13] The

development of simplified purification systems could allow the production of life-saving vaccines in-the-region-for-the-region. Scalability could be achieved through the growing vertical farming industry.

Toward these long-term goals, we set out to package samRNAs into plant virus-like particles (VLPs) derived from the plant viruses tobacco mosaic virus (TMV) and cowpea chlorotic mottle virus (CCMV). The plant virus nanotechnology is a unique platform offering several distinct advantages: VLPs derived from TMV, for example, are stable to high temperatures and in many solvents.[14] Accordingly, they do not require refrigeration during storage or distribution, freeing the resulting vaccine particles from reliance on the expensive and inconvenient cold chain. Further, VLPs are a particularly attractive platform for vaccine development because they are highly visible to the immune system, so the particles serve not only as a delivery vehicle but also as an adjuvant. Their highly organized and repetitive structures act as pathogen-associated molecular patterns (PAMPs), triggering the innate immune system through pattern recognition receptors (PRRs), most commonly toll-like receptors (TLRs).[15] While the proteinaceous capsids are recognized by TLR-2[16] (and likely other PRRs), RNA-containing VLPs also signal through TLR7/8.[17] These immune-stimulatory properties in combination with their size make them ideal candidates for vaccine delivery to the draining lymph nodes and for priming interactions with antigen-presenting cells (APCs).[18]

In this work, we tested side-by-side the assembly and delivery of VLPs that are *in vitro* reconstituted, alternately, from the viral coat proteins of TMV or CCMV and that contain self-replicating forms of fluorescent or luminescent mRNA genes.While each of CCMV[7] and TMV[19] capsid protein has been used for the delivery of self-amplifying mRNA genes in in vitro reconstituted VLPs, they have not previously been compared directly ‘head-to-head’. The nucleoprotein assemblies made from TMV coat proteins form high-aspect-ratio helical-symmetry cylinders, while CCMV coat proteins lead to icosahedrally symmetric spherical assemblies. The TMV tubes measure 18 nm in width and are up to 100s of nm long, the length being directly proportional to the length of the packaged RNA, whereas the CCMV spheres measure 28 nm in diameter. Expression levels of the packaged gene and the fate of the VLP carrier were determined through imaging studies in both *in vitro* (cell culture) and *in vivo* (mouse) models. More explicitly, the fate of the VLPs in the mouse, and in particular, trafficking to the draining lymph nodes following footpad injection, was monitored by fluorescence counts of harvested lymph nodes and by direct *in vivo* imaging of the lymph nodes.

MATERIALS AND METHODS

Cloning Strategy.

The plasmid constructs, pNod-Luc, and pNod-EYFP, coding for the self-amplifying Nodamura replicon (Nod) expressing Renilla luciferase (Luc) and enhanced yellow fluorescent protein (EYFP), respectively, were made from a gift from Raul Andino (University of California, San Francisco), described in Gitlin et al.[20] To promote packaging into TMV VLPs the TMV origin of assembly site (OAS, 234 nts)[21] was inserted downstream of the marker gene in the pNod-EYFP and pNod-Luc plasmids using *Age*I

and *BsI*WI restriction sites and yielding the following plasmids- pNod-EYFPOAS and pNod-LucOAS (Supporting Figure S1). Cloning was validated by sequencing.

In Vitro Transcription of the mRNA Cassettes.

The plasmid constructs were linearized by single digestion using *Xba*I at the 3′ end of the replicon. Linearized plasmids were then *in vitro* transcribed using T7 High Yield RNA Synthesis Kit (New England Biolabs, Ipswich, MA) or (MEGAscript T7 Transcription Kit, Thermo Fisher, Waltham, MA) as per manufacturer's instructions. The transcription was allowed to proceed in the presence of an RNase inhibitor (1 U/μL, Thermo Fisher Scientific, Waltham, MA) for 1–2 h at 37 °C in a heat block. After transcription, the plasmid DNA template was removed by enzymatic digestion using an RNase-free DNase I (2U, New England Biolabs, Ipswich, MA), which was incubated for 15 min at 37 °C. The transcribed mRNA constructs were purified using either LiCl precipitation or by using an RNEasy Mini Kit (Qiagen, Valencia, CA). For efficient translation, a 7-methylguanylate cap structure was added to the 5′ end of the mRNA using a vaccinia virus capping system (New England Biolabs, Ipswich, MA) and then purified using an RNEasy Mini Kit (Qiagen, Valencia, CA) following the manufacturers' specifications. The resulting mRNA cassettes (Nod.Luc, Nod.EYFP, Nod.LucOAS, and Nod.EYFPOAS) were then characterized by UV/vis Spectroscopy (Nanodrop 2000, Thermo Fisher, USA) to corroborate purity (only RNA with a A260/A280 ratio of within 2.0–2.2 was used). To confirm the size of the mRNA, constructs were characterized by agarose gel electrophoresis using a 0.85% (w/v) agarose gel in electrophoresis buffer (1× Tris-Acetate-EDTA (TAE) buffer, pH 8.0), and electropherograms were analyzed using an Agilent 2100 bioanalyzer. mRNA cassettes were stored at −80 °C until further use.

Preparation of TMV and CCMV Coat Proteins (CPs).

The TMV CP was prepared as previously described.[22] In brief, TMV was purified from the infected leaves of *Nicotiana benthamiana*. To prepare the CPs, 10 mg of TMV in potassium phosphate buffer (0.1 M KP, pH 7.4) was treated with 2 volumes of glacial acetic acid (34.8 M) for 20 min on ice. The mixture was centrifuged at 20 000*g* for 20 min at 4 °C, and the supernatant was collected and dialyzed against Milli-Q water for 48 h using a 6–8 kDa dialysis membrane (Spectra Por S/P 1 Dialysis Membrane; Thermo Fisher Scientific, Waltham, MA). CP was collected by centrifugation at 20 000*g* for 20 min at 4 °C followed by overnight resuspension of the white pellet in 75 mM sodium phosphate buffer, pH 7.2. The integrity of the coat protein was determined by UV/vis spectroscopy (Nanodrop 2000, Thermo Fisher Scientific, Waltham, MA) by measuring absorbance at 250 nm (for traces of contaminants-SDS or EDTA), 260 nm (for single-stranded RNA), 280 nm (for proteins containing Trp, Tyr or Cys-Cys disulfide bonds). The concentration of the TMV CP was determined at 260 nm using an extinction coefficient $\varepsilon = 1.3\ \mu L\ \mu g^{-1}\ cm^{-1}$.

CCMV CP was expressed and purified from a bacterial expression system. Chemically competent cells of *Escherichia coli* strain Rosetta 2 BL21 (New England Biolabs, Ipswich, MA) were transformed with the T7–7 × HisTag—CCMV CP construct for CCMV capsid protein expression. The transformed cells were grown in LB medium (Thermo Fisher Scientific, Waltham, MA) supplemented with ampicillin and chloramphenicol (Goldbio, St.

Louis, MO), at 37 °C with constant agitation until an optical density of 0.6 absorbance units was attained. Recombinant expression of the CCMV CP was induced after the addition of isopropyl-d-1-thiogalactopyranoside (IPTG) (Goldbio, St. Louis, MO), at a final concentration of 1 mM, and incubated for 16 h at 20 °C with constant stirring. Induced cells were collected by centrifugation at 15 000*g* for 10 min at 4 °C, with the pellet stored at −80 °C until purification. Cell Pellets were resuspended in salt lysis buffer (1 M NaCl, 50 mM Tris-HCl, and 5 mM TCEP) (Goldbio, St. Louis, MO). The resuspended cells were lysed by sonication and homogenized in an Emulsiflex (Avestin Emulsiflex C-3). The cell lysate was centrifuged at 12 000*g* for 45 min at 9 °C and the supernatant was collected. The protein was purified using the 7× histidine tag by running the cell lysate over a nickel resin column (Thermo Scientific, Waltham, MA) eluted with 50 mM imidazole (Thermo Scientific, Waltham, MA) and stored at 4 °C. The histidine tag was cleaved using pro-TEV protease overnight. Finally, the purified protein was dialyzed using a 6–8 kDa dialysis membrane (Spectra Por S/P 1 Dialysis Membrane; Thermo Fisher Scientific, Waltham, MA) into buffer B (1 M NaCl, 20 mM Tris pH 7.2, 1 mM EDTA, 1 mM DTT, 1 mM PMSF) (Millipore Sigma, St. Louis, MO) and aliquoted at 1 mg/mL. For further use, the protein was flash-frozen in liquid nitrogen and stored at −80 °C until ready to use, at which point it was defrosted on ice and stored at 4 °C for up to 2 weeks. The integrity of the CP was determined by UV/vis spectroscopy (Nanodrop 2000, Thermo Fisher Scientific, Waltham, MA) by measuring absorbance at 260 nm (for single-stranded RNA) and at 280 nm (for proteins containing Trp, Tyr, or Cys-Cys disulfide bonds). The concentration of the CCMV CP was determined at 280 nm and with $\varepsilon = 1.27\ \mu L\ \mu g^{-1}\ cm^{-1}$ (only CCMV CP with a 260/280 ratio of less than 0.62 was used for assembly).

In Vitro Self-Assembly of TMV and CCMV VLPs with mRNA Cassettes.

In vitro transcribed samRNAs were incubated with the TMV CP at a 20:1 protein/RNA mass ratio in resuspension buffer (Sodium phosphate buffer, pH 7.2) at 30 °C for 16–18 h. The assembled VLPs were treated with RNaseA (0.11:1 mass ratio RNaseA to RNA, Thermo Fisher Scientific, Waltham, MA) at 37 °C for 30 min, followed by purification of VLPs using 100 kDa Amicon spin column (Millipore Sigma, St. Louis, MO), or not RNaseA-treated. RNase degrades free samRNA that did not get assembled, as well as samRNA encapsidated into defective VLPs, and, in the case of CCMV VLPs, the RNA threaded between multiplets (see below). For this reason, non-RNaseA-treated VLPs were also tested. For assembly of CCMV VLPs, mRNAs were mixed with the CP at a protein/RNA mass ratio of 4.2 in protein storage buffer (1 M NaCl, 20 mM Tris pH 7.2, 1 mM EDTA, 1 mM DTT, 1 mM PMSF) and then dialyzed overnight for 12–16 h against RNA assembly buffer (50 mM Tris pH 7.2, 50 mM NaCl, 10 mM KCl, 5 mM $MgCl_2$, 1 mM DTT) at 4 °C. The VLPs were dialyzed again but now against virus suspension buffer (50 mM sodium acetate buffer pH 4.5, 8 mM magnesium acetate) at 4 °C for at least 6 h and finally either RNaseA-treated and purified with 100 kDa Amicon filters or used without any RNaseA treatment.

Characterization of mRNA-Containing VLPs.

UV/vis spectroscopy (NanoDrop 2000, Thermo Fisher Scientific, Waltham, MA) was used to check the integrity, purity, and concentration of the assembled VLPs. The structural

integrity of the VLPs was determined by transmission electron microscopy (TEM). VLPs (0.2 mg/mL) were deposited on glow-discharged carbon-coated copper (200-mesh) PELCO Pinpointer grids (Ted Pella, USA). After 1 min, the grids were blotted with Whatman filter paper and then stained with 2% (w/v) uranyl acetate (6 μL) for 1 min. Micrographs were acquired using a Tecnai G2 TF20 High-resolution electron microscope (FEI, Hillsboro, OR) with an accelerating voltage of 200 kV. Images were collected at 3–4 μm underfocus with a TIETZ F415MP 16-megapixel CCD camera (4000 × 4000 pixels, pixel size 15 μm). Then, the hydrodynamic diameters, size distribution, and polydispersity indices (PDI) of VLPs were determined by dynamic light scattering with a Zetasizer Nano ZSP Zen5600 instrument (Malvern Panalytical, Malvern, UK). The purity of VLPs was determined by their elution profiles on a KTA Explorer chromatography system equipped with a Superose6 Increase column (GE Healthcare, Chicago, Illinois).

Transfection of mRNA and mRNA-Containing VLPs.

Free mRNA, mRNA-containing VLPs that were not RNaseA-treated, and RNaseA-treated VLPs were transfected in BHK-21 cells (ATCC, USA) as follows: 80 000 cells were seeded 24 h prior to transfections (70–90% confluence) into 6-well plates in 500 μL of Dulbecco's modified Eagle's medium complete medium (DMEM, Thermo Fisher Scientific, Waltham, MA) with 10% (v/v) fetal bovine serum (FBS, Thermo Fisher Scientific, Waltham, MA) and 1% (w/v) penicillin/streptomycin (Thermo Fisher Scientific, Waltham, MA). Cells were transfected using 0.5 μg/well of mRNA or mRNA-containing VLPs (for the latter, the mass was normalized to the amount of mRNA) and 5 μL Lipofectamine 2000 (Thermo Fisher Scientific, Waltham, MA) according to the manufacturer's specification. Post transfection, EYFP expression was analyzed using fluorescence microscopy (EVOS FL Cell Imaging System, Waltham, MA) at 0, 8, 24, 48, 96, 72, and 120 h, by flow cytometry at 24 h, and by a fluorescence plate reader (Infinite M Plex Tecan instrument, Männedorf, ZH). Luciferase expression was quantified at 0, 8, 24, 48, 96, 72, and 120 h using a dual-luciferase reporter assay system (Promega, Madison, WI) and Pierce Renilla Luciferase Glow Assay Kit as described in the manual. The expression of luciferase was measured by using a luminometer (Infinite M Plex Tecan instrument, Männedorf, ZH). Each transfection experiment was performed in biological triplicate.

Quantitative RT-PCR.

To quantify the number of marker genes Luc and EYFP—with or without the Nodamura replicon, RNA was isolated from the transfected cell lysates at 0, 8, 24, 48, 96, 72, and 120 h post–transfection using an RNEasy Mini Kit (Qiagen, Valencia, CA). Similarly, RNA was isolated at 1, 24, and 48 h post transfection with mRNA-containing VLPs. Following RNA extraction cDNA synthesis was carried out using an RT^2 first-strand kit, (Qiagen, Valencia, CA). Quantitative RT-PCR was performed using RT^2 SYBR Green qPCR Mastermix (Qiagen, Valencia, CA) with Luc- and EYFP-specific primers (Luc forward 5′-TAACGCGGCCTCTTCTTATTT-3′/Luc reverse 5′-GATTTGCCTGATTTGCCCATAC-3′; and EYFP forward 5′-GCACAAGCTGGAGTACAACTA-3′/EYFP reverse 5′-TGTTGTGGCGGATCTTGAA-3′). For reference control, we used GPDH gene-specific primers (forward 5′- GACTTCAACAGTGACTCCCAC-3′ / reverse : 5′-TCTGTTGCTGTAGCCAAATTC-3′). RT-PCR was carried out using a Biorad CFX96

Real-Time System thermal cycler (Biorad, Hercules, CA). Thresholds generated by PCR were measured as mean CT values, and the relative marker gene expression or fold change was calculated by 2-ΔΔ CT values. Quantitative RT-PCR was performed in triplicate.

Flow Cytometry.

BHK-21 cells were transfected using either 0.5 μg/well mRNA with or without the Nodamura replicon; dose escalation studies were also performed using 0.05–1 μg/well mRNA with the Nodamura replicon. 80 000 cells per well were seeded, and 24 h post transfection, the cells were harvested using Gibco Cell Dissociation Buffer (Thermo Fisher Scientific, Waltham, MA), followed by washing and resuspension in 1 × PBS, pH 7.4 containing 2% (v/v) FBS. The resuspended cells were then immediately analyzed for fluorescence using a BD AccuriTM C6 Plus flow cytometer. The flow cytometry data were processed with FlowJo v10 software.

Synthesis and Characterization of Fluorescent VLPs.

TMV was modified at solvent-exposed Glu side chains, Glu97 and Glu106, located within the central channel of TMV; the chemistry was as previously established.[23] In brief, the carboxylates are modified with a carbodiimide cross-linker to introduce an alkyne functional group, followed by azide−alkyne cycloaddition reactions using copper-catalyzed click chemistry: TMV (5 mg/mL in 0.1 M HEPES, pH 7.0 buffer) was mixed with propargylamine (0.73 mg; 25 mol equiv) and ethyl dimethyl aminopropyl carbodiimide (EDC, 25 mg; 22.5 mol equiv). The reaction mixture was incubated at RT for 4 h followed by the second addition of EDC (25 mg; 45 molar equivalences) and incubated for 12 h in dark conditions at RT. TMV was purified by ultracentrifugation on a sucrose cushion (30% w/v) for 1 h at 50 000*g* (Beckman Optima MAX-XP with TLA-55 rotor). TMV-alkyne was collected by restoring the pellet overnight in 0.1 M HEPES, pH 7.0, at 4 °C. TMV-alkyne (1 mg/mL in 0.1 M HEPES, pH 7.0 buffer) was conjugated with sulfo-Cy5-azide (Luminoprobe, Cockeysville, MD) in the presence of 2 mM aminoguanidine, premixed 1 mM copper sulfate, 3.7 mM tris(benzyltriazolylmethyl) amine, and 2 mM L-ascorbic acid. The reaction was incubated at 4 °C for 24 h and then purified by ultracentrifugation on a sucrose cushion.

Fluorescent CCMV was obtained by labeling the solvent-exposed lysine side chains using sulfo-Cy5 *N*-hydroxysuccinimide NHS ester (Lumiprobe, Cockeysville, MD). Specifically, CCMV (2 mg/mL) was mixed with a 100 molar excess of sulfo-Cy5 NHS ester in 0.1 M HEPES, pH 7.0, 5 mM $MgCl_2$ buffer containing 10% (v/v) DMSO. The reaction was incubated overnight at 4 °C with gentle agitation. Labeled CCMV pellet was collected by ultracentrifugation on a 30% (w/v) sucrose cushion at 50 000*g* for 1 h. The fluorescent VLPs were then characterized by UV/vis spectroscopy (Nanodrop 2000, Thermo Fisher Scientific, Waltham, MA) and were analyzed in a (12%) NuPAGE protein gel (Thermo Fisher Scientific, Waltham, MA).

In Vivo Delivery and Expression of mRNA-Containing VLPs.

Animal studies were conducted with the approval of the Institutional Animal Care and Use Committee (IACUC) of the University of California, San Diego. Balb/c mice (Female, 6–7

weeks) were used. To image VLPs, fluorescently labeled VLPs TMV.Cy5 and CCMV.Cy5 were subcutaneously administered at 100 μg VLPs in 20 μL of PBS into the footpad. The trafficking of fluorescent VLPs was assessed at 0, 5, 8, 24, 48, 168, and 720 h—animals were sacrificed, and the popliteal lymph nodes were harvested and then imaged using IVIS (*in vivo* imaging system). The fluorescent signals from the VLPs in lymph nodes were counted within the region of interest (ROI). For reporter mRNA gene expression analysis, Nod-EYFPOAS TMV VLPs and Nod-EYFPOAS CCMV VLPs that were not RNaseA-treated were used. VLPs (100 μg in 20 μL of PBS) were subcutaneously administered into the footpad of the Balb/c mice (Female, 6–7 weeks), and fluorescent signals were captured by IVIS at 0, 1, 4, 8, 24, and 48 h. The images were acquired beginning 5 min after intraperitoneal substrate administration, and the fluorescent signals were captured within 1 s exposure time and analyzed with IVIS Living Image software, version 3.0. The ROI was drawn to assess the relative luminescent signal intensity.

RESULTS

In Vitro Transcribed mRNA Replicons are Efficiently Packaged into CCMV and TMV VLPs.

mRNA cassettes were designed as shown in Figures 1A and S1, from plasmids containing the self-amplifying Nodamura replicon and marker gene Renilla luciferase (Luc) or enhanced yellow fluorescent protein (EYFP). The corresponding Nod.EYFPOAS and Nod.LucOAS mRNA transcripts have lengths of 4433 and 4626 nt, respectively. To facilitate assembly into TMV VLPs, the origin of the assembly site (OAS) of the TMV genome has been inserted downstream of the marker gene. Specifically, a 234 nt-long OAS sequence was used that corresponds to the TMV genome between 5312 and 5546 bp.[21] Prior to *in vitro* transcription using a T7 transcription kit, plasmids were linearized by using *Xba*I (data not shown). Post-transcription, a 7-methylguanylate cap structure was added. While poly(A) tails confer stability to mRNA, we opted not to include one because the Nodamura replicon has been shown to be stable in the absence of a poly(A) tail due to the presence of a high degree of secondary structure formation.[24] The purity, integrity, and size of the mRNA cassettes were confirmed using a bioanalyzer (Figure S2), and the presence of each component of the mRNA cassettes, including the Nodamura replicon (RNA-1), marker genes, and the OAS sequence, was confirmed by sequencing the respective amplicon obtained by reverse transcription PCR (data not shown).

For encapsulation and packaging into VLPs, coat proteins (CPs) of TMV and CCMV were prepared. Free CP of TMV has an A260:280 nm ratio of 0.65, while assembled TMV VLPs have an absorbance ratio of A260:280 nm ratio of 1.2. The disassembled TMV CP gave an A260:280 nm ratio of 0.65 ± 0.03, therefore indicating that pure CP of TMV was obtained. The purity and integrity of the CP were also confirmed by electron microscopy. TEM imaging was performed, confirming the presence of proteins and disks (Figure S3). CCMV CP was obtained by bacterial expression and characterization by UV−vis spectroscopy. The A260:280 nm ratio of monodispersed CP of CCMV should be 0.62 and we confirmed the generation of pure CCMV CP with an A260:280 nm absorbance ratio of ~0.6 ± 0.04; assembled CCMV nucleoprotein (VLP) has an A260:280 nm absorbance ratio of ~1.52. The coat proteins of TMV and CCMV were then used for VLP assembly: mRNA cassettes were

added to TMV and CCMV at protein-to-RNA mass ratios of 20:1 and 4.2:1, respectively, and assembly was allowed to proceed for 16–18 h for TMV and 24 h for CCMV.

TMV and CCMV nanoparticles containing Nod.LucOAS or Nod.EYFPOAS constructs were analyzed by TEM. For TMV the characteristic high-aspect cylinders were detected for the RNase-treated particles: Nod.LucOAS-containing TMV VLPs measured ~226 nm in length, and Nod.EYFPOAS-containing TMV VLPs were ~216 nm long (Figure 1B). The size difference reflects the different mRNA cassette length, the RNA serving as a template that guides the length of TMV VLP.[25] More explicitly, the nt-lengths of the EYFP and Luc constructs are 4433 and 4626 nt, having the same ratio (0.96) to one another as the measured lengths (216 and 226 nm) of the corresponding VLPs. Also for CCMV, intact VLPs were detected post assembly and the icosahedral nanoparticles measured 28–29 nm in diameter independent of the mRNA cassette (Figure 1B). We observed mostly singlets for RNase-treated CCMV VLPs (Figure 1B), while for *non*-RNase-treated assembly mixes a significant fraction of doublet CCMV particles were observed, involving the sharing of an RNA molecule by two capsids (Figure 1C). This is consistent with earlier observations in which multiplets of CCMV capsids begin to be observed when the packaged mRNA is longer than 3500 nts.[26] It should be noted that, unlike the case of TMV assembly, RNA packaging by CCMV capsid protein does not depend on the presence of a specific packaging signal.[27]

Finally, the RNA degradation of assembled VLPs treated or not treated with RNaseA was studied (Figure 1D). mRNA was extracted from assembled VLPs and run in agarose gels with degradation efficiency defined as the fraction of intensity in the Figure 1D densitometry traces that corresponds to the full-length molecule. While both RNase-treated and *non*-RNase-treated TMV VLPs correspond to essentially no degradation, RNase-treated CCMV VLPs showed almost complete (>90%) degradation of encapsulated RNA for the EYFP and Luc constructs. This reflects the fact that CCMV assemblies involve predominantly multiplets with RNase-accessible RNA; in contrast: TMV forms a single high-aspect-ratio nucleoprotein complex that efficiently protects its RNA cargo of any length.

EYFPOAS and LucOAS Replicons Are Active upon Transfection into BHK Cells and Significantly Enhance mRNA Expression.

Lipofectamine-mediated transfection delivering self-amplifying EYFP mRNA—the Nod.EYFPOAS replicon—was initially evaluated by fluorescence microscopy in various cell lines such as Hela, HEK293TT, HepG, and BHK-21 and we observed the highest expression of the protein in BHK-21 cells, confirming the integrity and activity of the mRNA replicon cassettes (data not shown). Dose-dependent studies were performed, and we determined 500 ng Nod-mRNA per 80 000 cells to be the ideal dose achieving maximum expression as determined by fluorescence microscopy, flow cytometry, and luciferase assay (Figure S4A–C), in agreement with earlier work.[28] Next, we compared the expression yields and kinetics of EYFP and Luc in their mRNA and samRNA forms. We observed protein expression for up to 120 h and quantified how much it is enhanced by fusing the mRNA to Nodamura replicase (Figure 2A–C). The microscopy results are consistent with the data from flow cytometry measurements showing that ~50% of the cells were positive for EYFP

expression post-transfection using Nod.EYFP mRNA while only ~32% of the cells were fluorescent when transfected with EYFP alone: the addition of the replicase significantly enhances target gene expression ($p < 0.05$; Figure 2B). We also used real-time quantitative PCR to assay the relative levels of EYFP and Luc mRNA, with or without the Nodamura replicon, confirming higher multifold change from 24 to 120 h for both the marker genes in the presence of replicon (Figure 2C), in agreement with earlier work.[7] Finally, RT-PCR analysis from the RNA isolated from the transfected cell lysates confirmed the transfection of mRNA cassettes with amplified bands of their expected sizes (~653 bp EYFP; ~886 bp Luc), as observed on the agarose gel (Figure S5).

Transfected Replicon-Containing CCMV and TMV VLPs Result in Downstream Protein Expression.

Next, we assessed the expression efficiency when the mRNA cassettes were lipofected into BHK-21 cells in the RNase-treated VLP form. Unlike other cell types in culture that are reported to take up CCMV VLPs without the mediation of transfection agent,[29] BHK cells require lipofectamine or electroporation. Accordingly, we used lipofectamine for all of our cell transformations, transfecting equivalent amounts of naked RNA and RNase-treated or *non*-RNase-treated CCMV or TMV VLPs. For mRNA-containing TMV VLPs, significant protein expression levels were achieved but only when the RNA was in replicon form, consistent with the effects of self-replication found in the naked mRNA transfection experiments reported above. Expression of luciferase was detectable when Nod.lucOAS was delivered in RNase-treated CCMV VLPs, but expression levels were not significant (Figure 3A,B); this is because for RNA of this length a dominant fraction of the assembly products are doublets of capsids that provide marginal protection against the strength of RNase treatment involved here (29). The amount of RNaseA used, however, is significantly higher (6×) than that present in blood serum (~0.5 ng/μL, comparable to a 0.02:1 RNaseA/RNA mass ratio for the volume used in our experiments), and we have shown that the RNA in CCMV multiplets is indeed protected against digestion (Duran Meza A.L, Porak S., Chapman A., Knobler C.M, Gelbart W.M. “Determination of an RNA Length Threshold for Efficient Encapsidation and RNaseA Protection by Cowpea Chlorotic Mottle Virus Coat Proteins Assembled into Virus-like Particles” Unpublished manuscript) for nuclease concentrations up to a mass ratio of 0.09:1 RNaseA to RNA, more than 4× that in blood serum. Accordingly, the experiments we report here were performed with *non*-RNase-treated VLP assemblies as well as RNase-treated ones. For TMV-based delivery of the mRNA cassettes, while efficient expression of the target gene was achieved the levels were lower when compared to those of naked mRNA. In particular, for EYFP mRNA they were 3.9-, 2.5-, and 3.3-fold lower at 24, 48, and 72 h post-transfection ($p < 0.0001$ at 24 and 48 h, and $p < 0.05$ at 72 h); for Luc mRNA, expression levels were 41.2- and 29.4-fold lower at 24 h ($p < 0.05$) and 48 h ($p < 0.005$). This is not surprising because in these lipofections the naked mRNA can be directly translated, while the VLP-packaged mRNA requires unloading from TMV. This “price” of delivering the RNA in VLP form, however, is more than compensated for by the level of protection provided against nuclease degradation, both for storage/handling purposes and, more significantly, for *in vivo* use: as we report in the next section, when naked mRNA replicon is injected into mice, there is no downstream gene expression in lymph nodes, in contrast to strong signals reported for VLP-packaged

replicon. In the case of RNaseA-treated CCMV VLPs the protein expression is very low, as expected since the percentage of surviving full-length mRNA was close to 0 (Figure 3A,B); on the other hand, the expression of the reporter gene following transfection of the *non*-RNaseA-treated CCMV VLPs is comparable with the expression of the naked RNA (Figure 4). Further, as we report in the next section, *non*-RNaseA-treated CCMV VLPs also survive when injected into mice, giving strong *in situ* (lymph node) protein expression.

VLPs Are Active in Lymph Nodes Resulting in Transgene Expression, Following Footpad Injection in Mice.

Next, we assayed trafficking of the VLPs *in vivo*—specifically, fluorescently labeled VLPs were administered into footpads of mice, and whole body as well as *ex vivo* imaging was carried out using IVIS (Figure S6A). VLP trafficking to and accumulation in the draining lymph nodes (dLNs) and the popliteal lymph nodes, was apparent. Significant levels of fluorescence in the dLNs were observed as early as 5 h post administration of VLPs, with maximum fluorescence counts observed at 24 h for both VLPs (Figure 5). Both TMV and CCMV signals were observed for over 168 h (Figure 5), while TMV signals gradually decreased after 24 h, strong CCMV signals were observed for up to 720 h post administration of the VLPs (Figures 4 and S6B). Significant differences between the two nanoparticle systems were apparent: CCMV showed more effective dLN homing with stronger signals observed throughout the study; in particular, the residence time within the dLNs was significantly increased ($p < 0.0001$ from 5 to 168 h for CCMV and $p < 0.05$ at 5 h, $p < 0.0001$ at 24 and 168 h, and $p < 0.005$ at 48 h for TMV). These differences most likely are a result of the different nanoparticle shapes (see the Discussion section).

Lastly, we assayed delivery and expression of Nod-mRNA-encapsulated TMV.Nod.EYFPOAS and CCMV.Nod.EYFPOAS VLPs, both without RNaseA treatment, to ensure the integrity of the mRNA. EYFP expression was confirmed for Nod.EYFP mRNA-delivered by TMV and CCMV: EYFP signals in the dLNs were detectable as early as 4 h post administration (Figure 6) and significant signals remained detectable over 8 h post administration (Figure 6) but decreased gradually over extended time periods. While the VLP-delivered mRNA led to effective transgene delivery, independent of the carrier, free mRNA did not yield any detectable protein levels as measured by IVIS. These data suggest that the VLPs (even the CCMV multiplets) significantly protect the encapsulated mRNA from RNases and enable lymphocyte homing and cell uptake. Further, they indicate that these particles, once in the cytoplasm of targeted cells, make their RNA content accessible to the ribosomal machinery, resulting in strong levels of mRNA translation and protein expression.

DISCUSSION

The present study has focused on evaluating the efficiencies of packaging and delivery of self-amplifying mRNA in spherical and cylindrical virus-like particles reconstituted, respectively, from the purified capsid protein of CCMV and TMV viruses. The role of an insect virus [Nodamura (Nod)] RNA replicase in therapeutic replicons has been explored earlier in mammalian cells, and T-cell responses have been reported in mouse models with

antigen-expressing short (<3.6 knt) Nod replicons packaged in spherical CCMV VLPs.[7] Here we consider longer (~4.5 knt) replicons and package them separately in spherical CCMV and cylindrical TMV VLPs, in order to compare for the first time the effect of particle geometry on packaging and delivery of self-amplifying mRNA genes in cell culture and in animal models. These replicons are as long as they are, even with the relatively short (3.2 knt) Nod replicase gene, because of the 720 and 936 nt reporter genes involved and the requisite 234 nt OAS sequence but are still as short as a gene- and OAS-containing one-molecule replicon can be. Longer RNAs have the unavoidable drawbacks of greater cytotoxicity due to the formation of dsRNA[11,30] and pose higher probability of undesirable mutations that may lead to unstable/toxic clones in bacteria (such as the 25–32knt constructs of *Coronaviridae*).[31] Two-molecule replicon systems have been employed in which the RNA replicase works in trans to amplify the gene of interest,[32] but the level of amplification is necessarily lower. Accordingly, we choose to work with the short replicase gene of Nodamura[20] for the evaluation of gene packaging and efficiencies.

The assembly of infectious virus particles in a test tube is unique to a few single-stranded RNA (ssRNA) plant viruses, notably the cowpea chlorotic mottle virus (CCMV), brome mosaic virus (BMV), and tobacco mosaic virus (TMV). These viruses have been shown to self-assemble *in vitro*[33] and are of interest as delivery vehicles for therapeutics.[34] CCMV CP assembles *in vitro* around nonviral RNA in a two-step protocol resulting in spherical, monodisperse, 28 nm icosahedral VLPs.[35] When the RNA length is between 2500 and 3500 nts, a single RNA molecule is packaged into one 28 nm-VLP, with relative efficiency depending on length and sequence.[26] However, when the RNA is longer than 3500 nts, the RNA is packaged into two or more 28 nm-sized VLPs with the RNA shared between the particles.[26] TMV, on the other hand, assembles *in vitro* to form hollow, helical rod-like VLPs.[36] The rods have an inner diameter of 4 nm and an outer diameter of 18 nm with the length of the rod depending on the length of the RNA being packaged.[25,36] The packaged RNA forms a helix that is embedded about 2 nm into the protein shell, whose subunits are ordered into a helix with the same pitch as the RNA helix, with 3 RNA nts per capsid protein. Further, TMV CP can encapsulate nonviral RNA of any length if the RNA contains a specific recognition sequence, or packaging signal, the origin of assembly site (OAS), at which VLP nucleation begins.[21] More explicitly, the nucleation of 17.5 kDa coat protein initiates in the presence of 6.4 knt TMV genomic RNA to form a 300 nm × 18 nm rod shaped filament of 2130 identical copies of coat protein.[36] The assembly of 4.4 and 4.6 knt saNod-mRNA with TMV coat proteins results in rods with the same 18 nm diameter but with lengths of 206 nm $\left(=\frac{4.4}{6.4}300\,\mathrm{nm}\right)$ and 216 nm $\left(=\frac{4.6}{6.4}300\,\mathrm{nm}\right)$, as observed.

The trafficking of therapeutic RNA-loaded VLPs within the cellular uptake pathway is essential for an effective mRNA delivery particle. In particular, mRNA vaccine particles are primarily transported to lysosomes through the clathrin-mediated or micropinocytosis-dependent endosomal pathway,[37] but it is necessary that they escape the lysosome to achieve high transfection efficiency within the cytoplasm.[38] Our data indicate the presence of VLPs in the cytoplasm, and this is consistent with the observed transgene expression. Further, the data show that the VLP systems enable cell uptake and trafficking, as well as mRNA cargo release and expression. The VLPs also confer stability and protection from

premature enzymatic degradation with significant differences found for TMV and CCMV: RNase-treated TMV-VLP-mediated delivery of saNod-mRNA both *in vitro* as well as *in vivo* resulted in significant expression of marker genes, whereas distinctly less protein expression was observed when the same self-amplifying gene was delivered using RNaseA-treated CCMV VLPs. This difference is due to the degradation of the RNA occurring during RNaseA treatment because of the RNA being too long to be packaged and protected by a single CCMV capsid so that it is vulnerable to digestion along its length that is threaded between two capsids in a doublet structure. On the other hand, the *non*-RNaseA-treated CCMV VLPs do show in vivo expression of the reporter gene, whereas injection of the same number of molecules of (*non*-RNase-treated) naked mRNA does not. This is because *in vivo* RNase concentrations are lower than in our experimental design so that mRNA cargo delivered by CCMV multiplets was indeed observed, whereas injection of naked/unpackaged mRNA did not result in downstream gene activity.

The efficacy of any vaccine primarily depends on the targeted delivery of antigen to lymphoid organs for activating antigen-presenting cells and stimulating immune responses. The cellular uptake and trafficking demonstrated here for self-amplifying-RNA-loaded VLPs in the draining lymph node indicate the potential for developing corresponding mRNA vaccine delivery tools. However, the trafficking of VLPs depends on their geometry/morphology: the 28 nm CCMV VLPs show free migration to the popliteal lymph node within 5 h of injection, while the migration rate of TMV is significantly slower. Maximal retention of both VLPs was observed at 24 h and subsequently retained for 168 h. Recent reports on the interaction of VLPs with antigen-presenting cells and their role as adjuvant in generating protective immune response in animal models[39] also confirm the potential of VLPs as mRNA nanotechnology vaccine delivery tools. The present study highlights the particular delivery advantages of *in vitro* reconstituted spherical and rod-like VLPs formed from plant virus capsid protein and self-amplifying mRNA.

Supplementary Material

Refer to Web version on PubMed Central for supplementary material.

ACKNOWLEDGMENTS

This work was funded in part through grants from the NIH (R21 AI161306 to N.F.S.) and NSF (CBET-2134535 to N.F.S. and DMR-2011924, UC San Diego MSREC, and MCB-2103700 to W.M.G.). The authors thank Dr. Adam Biddlecome (UCLA) for making the plasmid constructs.

REFERENCES

(1). (a)Day M Covid-19: four fifths of cases are asymptomatic, China figures indicate. BMJ 2020, 369, m1375. [PubMed: 32241884] (b)Mizumoto K; Kagaya K; Zarebski A; Chowell G Estimating the asymptomatic proportion of coronavirus disease 2019 (COVID-19) cases on board the Diamond Princess cruise ship, Yokohama, Japan, 2020. Eurosurveillance 2020, 25 (10), 2000180. [PubMed: 32183930] (c)Sutton D; Fuchs K; D'Alton M; Goffman D Universal Screening for SARS-CoV-2 in Women Admitted for Delivery. N. Engl. J. Med 2020, 382, 2163–2164, DOI: 10.1056/NEJMc2009316. [PubMed: 32283004]

(2). Chaudhary N; Weissman D; Whitehead KA mRNA vaccines for infectious diseases: principles, delivery and clinical translation. Nat. Rev. Drug Discovery 2021, 20 (11), 817–838. [PubMed: 34433919]

(3). (a)Lorentzen CL; Haanen JB; Met Ö; Svane IM Clinical advances and ongoing trials on mRNA vaccines for cancer treatment. Lancet Oncol. 2022, 23 (10), e450–e458, DOI: 10.1016/S1470-2045(22)00372-2. [PubMed: 36174631] (b)Bejar N; Tat TT; Kiss DL RNA Therapeutics: the Next Generation of Drugs for Cardiovascular Diseases. Curr. Atheroscler. Rep 2022, 24 (5), 307–321, DOI: 10.1007/s11883-022-01007-9. [PubMed: 35364795] (c)Dhaliwal HK; Fan Y; Kim J; Amiji MM Intranasal Delivery and Transfection of mRNA Therapeutics in the Brain Using Cationic Liposomes. Mol. Pharmaceutics 2020, 17 (6), 1996–2005 From NLM..

(4). Kim SC; Sekhon SS; Shin WR; Ahn G; Cho BK; Ahn JY; Kim YH Modifications of mRNA vaccine structural elements for improving mRNA stability and translation efficiency. Mol. Cell. Toxicol 2022, 18 (1), 1–8, DOI: 10.1007/s13273-021-00171-4. [PubMed: 34567201]

(5). Blakney AK; Ip S; Geall AJ An Update on Self-Amplifying mRNA Vaccine Development. Vaccines 2021, 9 (2), 97 DOI: 10.3390/vaccines9020097. [PubMed: 33525396]

(6). Bloom K; van den Berg F; Arbuthnot P Self-amplifying RNA vaccines for infectious diseases. Gene Ther. 2021, 28 (3–4), 117–129, DOI: 10.1038/s41434-020-00204-y. [PubMed: 33093657]

(7). Biddlecome A; Habte HH; McGrath KM; Sambanthamoorthy S; Wurm M; Sykora MM; Knobler CM; Lorenz IC; Lasaro M; Elbers K; Gelbart WM Delivery of self-amplifying RNA vaccines in in vitro reconstituted virus-like particles. PLoS One 2019, 14 (6), No. e0215031. [PubMed: 31163034]

(8). Lundstrom K Self-Replicating RNA Viruses for Vaccine Development against Infectious Diseases and Cancer. Vaccines 2021, 9 (10), 1187 DOI: 10.3390/vaccines9101187. [PubMed: 34696295]

(9). Travieso T; Li J; Mahesh S; Mello JD; Blasi M The use of viral vectors in vaccine development. npj Vaccines 2022, 7 (1), 75. [PubMed: 35787629]

(10). Diken M; Kranz LM; Kreiter S; Sahin U mRNA: A Versatile Molecule for Cancer Vaccines. Curr. Issues Mol. Biol 2017, 22, 113–128, DOI: 10.21775/cimb.022.113. [PubMed: 27801664]

(11). Ceppi M; Ruggli N; Tache V; Gerber H; McCullough KC; Summerfield A Double-stranded secondary structures on mRNA induce type I interferon (IFN alpha/beta) production and maturation of mRNA-transfected monocyte-derived dendritic cells. J. Gene Med 2005, 7 (4), 452–465, DOI: 10.1002/jgm.685. [PubMed: 15515120]

(12). Wilson B; Geetha KM Lipid nanoparticles in the development of mRNA vaccines for COVID-19. J. Drug Delivery Sci. Technol 2022, 74, 103553 DOI: 10.1016/j.jddst.2022.103553.

(13). Chung YH; Church D; Koellhoffer EC; Osota E; Shukla S; Rybicki EP; Pokorski JK; Steinmetz NF Integrating plant molecular farming and materials research for next-generation vaccines. Nat. Rev. Mater 2022, 7 (5), 372–388. [PubMed: 34900343]

(14). Shirbaghaee Z; Bolhassani A Different applications of virus-like particles in biology and medicine: Vaccination and delivery systems. Biopolymers 2016, 105 (3), 113–132, DOI: 10.1002/bip.22759. [PubMed: 26509554]

(15). Bachmann MF; Jennings GT Vaccine delivery: a matter of size, geometry, kinetics and molecular patterns. Nat. Rev. Immunol 2010, 10 (11), 787–796. [PubMed: 20948547]

(16). Shepardson KM; Schwarz B; Larson K; Morton RV; Avera J; McCoy K; Caffrey A; Harmsen A; Douglas T; Rynda-Apple A Induction of Antiviral Immune Response through Recognition of the Repeating Subunit Pattern of Viral Capsids Is Toll-Like Receptor 2 Dependent. MBio 2017, 8 (6), 10–1128, DOI: 10.1128/mBio.01356-17.

(17). (a)Albakri MM; Veliz FA; Fiering SN; Steinmetz NF; Sieg SF Endosomal toll-like receptors play a key role in activation of primary human monocytes by Cowpea Mosaic Virus. Immunology 2020, 159, 183–192, DOI: 10.1111/imm.13135. [PubMed: 31630392] (b)Carignan D; Herblot S; Laliberte-Gagne ME; Bolduc M; Duval M; Savard P; Leclerc D Activation of innate immunity in primary human cells using a plant virus derived nanoparticle TLR7/8 agonist. Nano-medicine 2018, 14 (7), 2317–2327.

(18). Link A; Zabel F; Schnetzler Y; Titz A; Brombacher F; Bachmann MF Innate immunity mediates follicular transport of particulate but not soluble protein antigen. J. Immunol 2012, 188 (8), 3724–3733. [PubMed: 22427639]

(19). Maharaj P; Mallajosyula J; Lee G; Thi P; Zhou Y; Kearney C; McCormick A Nanoparticle Encapsidation of Flock House Virus by Auto Assembly of Tobacco Mosaic Virus. Int. J. Mol. Sci 2014, 15, 18540. [PubMed: 25318056]

(20). Gitlin L; Hagai T; Labarbera A; Solovey M; Andino R Rapid Evolution of Virus Sequences in Intrinsically Disordered Protein Regions. PLoS Pathog. 2014, 10 (12), No. e1004529, DOI: 10.1371/journal.ppat.1004529. [PubMed: 25502394]

(21). Saunders K; Thuenemann EC; Peyret H; Lomonossoff GP The Tobacco Mosaic Virus Origin of Assembly Sequence is Dispensable for Specific Viral RNA Encapsidation but Necessary for Initiating Assembly at a Single Site. J. Mol. Biol 2022, 434 (24), No. 167873, DOI: 10.1016/j.jmb.2022.167873. [PubMed: 36328231]

(22). Lam P; Gulati NM; Stewart PL; Keri RA; Steinmetz NF Bioengineering of Tobacco Mosaic Virus to Create a Non-Infectious Positive Control for Ebola Diagnostic Assays. Sci. Rep 2016, 6 (1), No. 23803. [PubMed: 27030058]

(23). Bruckman MA; Steinmetz NF Chemical modification of the inner and outer surfaces of Tobacco Mosaic Virus (TMV). Methods Mol. Biol 2014, 1108, 173–185. [PubMed: 24243249]

(24). Newman JFE; Brown F Absence of poly (A) from the infective RNA of Nodamura virus. J. Gen. Virol 1976, 30 (1), 137–140, DOI: 10.1099/0022-1317-30-1-137. [PubMed: 173797]

(25). Shukla S; Eber FJ; Nagarajan AS; DiFranco NA; Schmidt N; Wen AM; Eiben S; Twyman RM; Wege C; Steinmetz NF The Impact of Aspect Ratio on the Biodistribution and Tumor Homing of Rigid Soft-Matter Nanorods. Adv. Healthcare Mater 2015, 4 (6), 874–882, DOI: 10.1002/adhm.201400641.

(26). Cadena-Nava RD; Comas-Garcia M; Garmann RF; Rao AL; Knobler CM; Gelbart WM Self-assembly of viral capsid protein and RNA molecules of different sizes: requirement for a specific high protein/RNA mass ratio. J. Virol 2012, 86 (6), 3318–3326. [PubMed: 22205731]

(27). Wege C; Koch C From stars to stripes: RNA-directed shaping of plant viral protein templatesstructural synthetic virology for smart biohybrid nanostructures. Wiley Interdiscip. Rev.: Nanomed. Nanobiotechnol 2020, 12 (2), No. e1591, DOI: 10.1002/wnan.1591. [PubMed: 31631528]

(28). Tanimoto CR; Thurm AR; Brandt DS; Knobler CM; Gelbart WM The Nonmonotonic Dose Dependence of Protein Expression in Cells Transfected with Self-Amplifying RNA. J. Virol 2022, 96 (7), No. e01858–21, DOI: 10.1128/jvi.01858-21. [PubMed: 35293773]

(29). Villagrana-Escareño MV; Reynaga-Hernandez E; Galicia-Cruz OG; Duran-Meza AL; De la Cruz-Gonzalez V; Hernandez-Carballo CY; Ruiz-Garcia J VLPs Derived from the CCMV Plant Virus Can Directly Transfect and Deliver Heterologous Genes for Translation into Mammalian Cells. Biomed. Res. Int 2019, 2019, No. 4630891. [PubMed: 31781617]

(30). (a)Bryant JD; Lee JS; De Almeida A; Jacques J; Chang C-H; Fassler W; Quéva C; Lerner L; Kennedy EM Seneca Valley Virus replicons are packaged in trans and have the capacity to overcome the limitations of viral transgene expression. Mol. Ther.–Oncolytics 2023, 28, 321–333, DOI: 10.1016/j.omto.2023.02.005. [PubMed: 36938543] (b)McCullough KC; Milona P; Thomann-Harwood L; Démoulins T; Englezou P; Suter R; Ruggli N Self-Amplifying Replicon RNA Vaccine Delivery to Dendritic Cells by Synthetic Nanoparticles. Vaccines 2014, 2 (4), 735–754, DOI: 10.3390/vaccines2040735. [PubMed: 26344889]

(31). (a)Tews BA; Meyers G Self-Replicating RNA. RNA Vaccines: Methods Mol. Biol 2017, 1499, 15–35, DOI: 10.1007/978-1-4939-6481-9_2. [PubMed: 27987141] (b)Fernandes RS; Freire M; Bueno RV; Godoy AS; Gil L; Oliva G Reporter Replicons for Antiviral Drug Discovery against Positive Single-Stranded RNA Viruses. Viruses 2020, 12 (6), 598 DOI: 10.3390/v12060598. [PubMed: 32486283]

(32). Beissert T; Perkovic M; Vogel A; Erbar S; Walzer KC; Hempel T; Brill S; Haefner E; Becker R; reci Ö; Sahin U A Trans-amplifying RNA Vaccine Strategy for Induction of Potent Protective Immunity. Mol. Ther 2020, 28 (1), 119–128, DOI: 10.1016/j.ymthe.2019.09.009. [PubMed: 31624015]

(33). Buzón P; Maity S; Roos WH Physical virology: From virus self-assembly to particle mechanics. Wiley Interdiscip. Rev.: Nanomed. Nanobiotechnol 2020, 12 (4), No. e1613, DOI: 10.1002/wnan.1613. From NLM. [PubMed: 31960585]

(34). (a)Chung YH; Cai H; Steinmetz NF Viral nanoparticles for drug delivery, imaging, immunotherapy, and theranostic applications. Adv. Drug Delivery Rev 2020, 156, 214–235. (b)Ikwuagwu B; Tullman-Ercek D Virus-like particles for drug delivery: a review of methods and applications. Curr. Opin. Biotechnol 2022, 78, 102785 DOI: 10.1016/j.copbio.2022.102785. [PubMed: 36099859]

(35). Azizgolshani O; Garmann RF; Cadena-Nava R; Knobler CM; Gelbart WM Reconstituted plant viral capsids can release genes to mammalian cells. Virology 2013, 441 (1), 12–17. [PubMed: 23608360]

(36). Lomonossoff GP; Wege C TMV Particles: The Journey From Fundamental Studies to Bionanotechnology Applications. Adv. Virus Res 2018, 102, 149–176. [PubMed: 30266172]

(37). Fan N; Chen K; Zhu R; Zhang Z; Huang H; Qin S; Zheng Q; He Z; He X; Xiao W; et al. Manganese-coordinated mRNA vaccines with enhanced mRNA expression and immunogenicity induce robust immune responses against SARS-CoV-2 variants. Sci. Adv 2022, 8 (51), No. eabq3500. From NLM. [PubMed: 36563159]

(38). Wu Z; Li T Nanoparticle-Mediated Cytoplasmic Delivery of Messenger RNA Vaccines: Challenges and Future Perspectives. Pharm. Res 2021, 38 (3), 473–478, DOI: 10.1007/s11095-021-03015-x. [PubMed: 33660201]

(39). (a)Zepeda-Cervantes J; Ramírez-Jarquín JO; Vaca L Interaction Between Virus-Like Particles (VLPs) and Pattern Recognition Receptors (PRRs) From Dendritic Cells (DCs): Toward Better Engineering of VLPs. Front. Immunol 2020, 11, 529088 DOI: 10.3389/fimmu.2020.01100. (b)Nooraei S; Bahrulolum H; Hoseini ZS; Katalani C; Hajizade A; Easton AJ; Ahmadian G Virus-like particles: preparation, immunogenicity and their roles as nanovaccines and drug nanocarriers. J. Nanobiotechnol 2021, 19 (1), 59 DOI: 10.1186/s12951-021-00806-7.

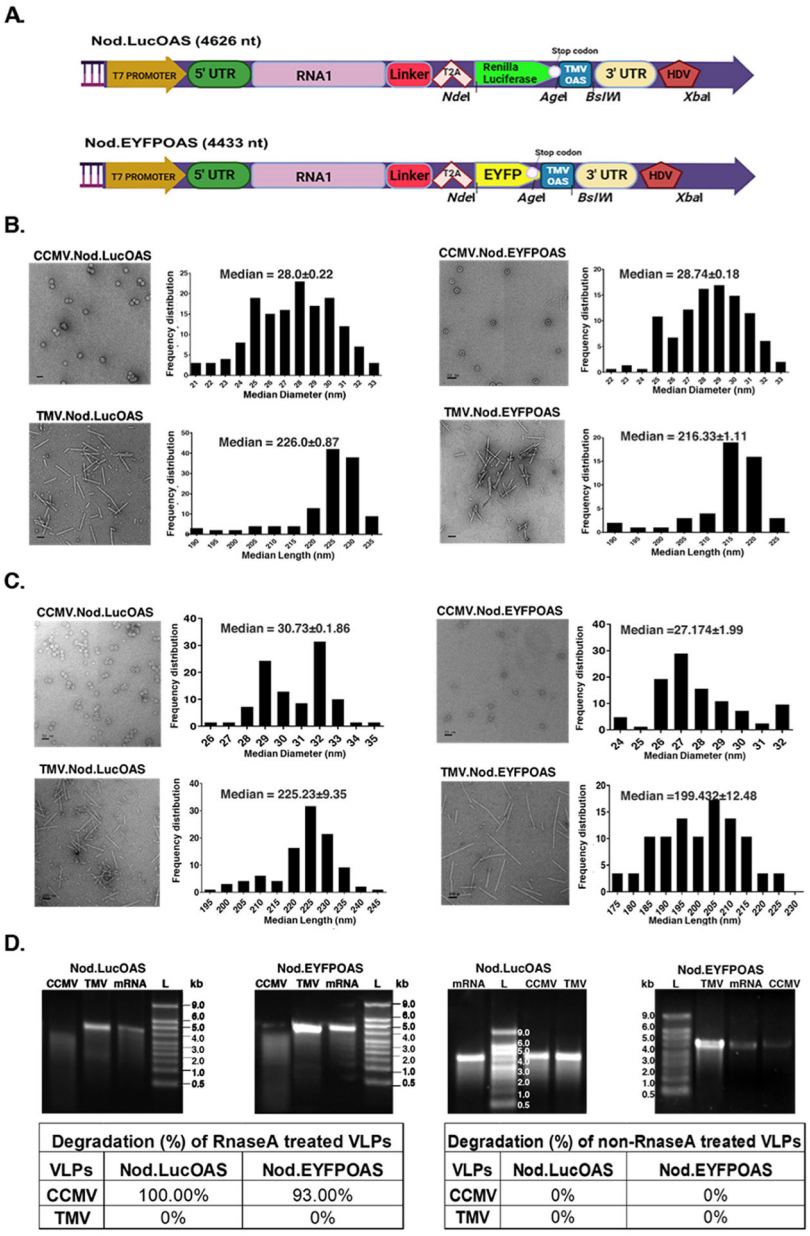

Degradation (%) of RnaseA treated VLPs		
VLPs	Nod.LucOAS	Nod.EYFPOAS
CCMV	100.00%	93.00%
TMV	0%	0%

Degradation (%) of non-RnaseA treated VLPs		
VLPs	Nod.LucOAS	Nod.EYFPOAS
CCMV	0%	0%
TMV	0%	0%

Figure 1.

(A) Schematic of the mRNA cassettes created by using Biorender. (B) Electron micrographs, median diameters, and lengths of RNaseA-treated CCMV and TMV VLPs containing Nod.LucOAS and Nod.EYFPOAS mRNA cassettes. (C) Electron micrographs and median diameters and lengths of *non*-RNaseA-treated CCMV and TMV VLPs containing Nod.LucOAS and Nod.EYFPOAS mRNA cassettes. (D) Agarose electrophoresis gels (0.85% in 1 × TAE, pH 8.0) of RNA extracted post RNase treatment and without RNase treatment from Nod.LucOAS and Nod.EYFPOAS mRNA-containing CCMV and TMV VLPs. The lane labeled “mRNA” is the *in vitro* transcribed RNA used in the assembly reactions. The extent (percentage) of degraded RNA extracted from RNase- and *non*-RNase-treated VLPs is determined from the density of RNA bands analyzed using ImageJ software.

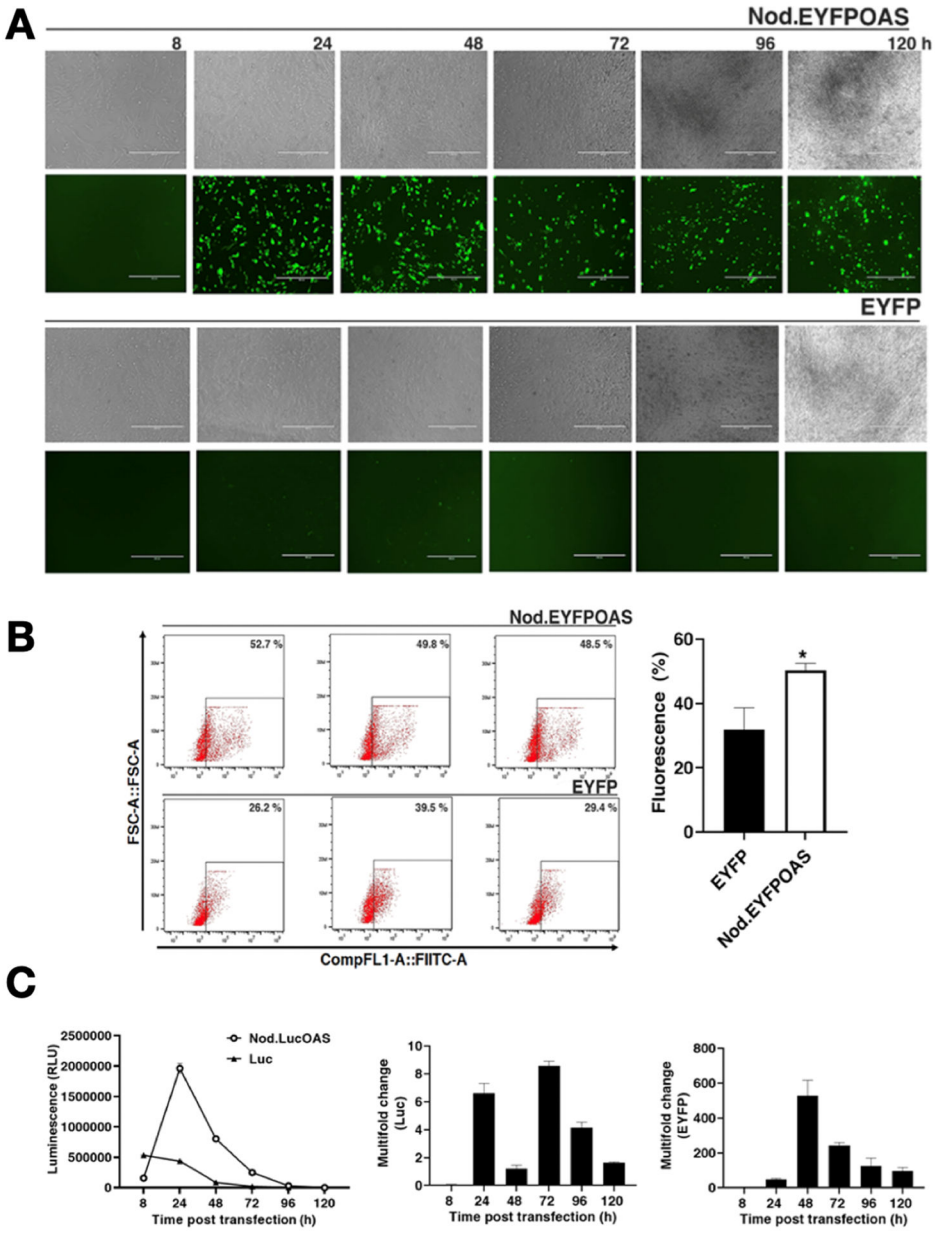

Figure 2.

Expression of reporter genes upon transfection into BHK cells of 500 ng of mRNA in *non*-self-amplifying (EYFP and Luc) and self-amplifying/replicon (Nod.EYFPOAS and Nod.LucOAS) form, using lipofectamine seeded into the 6-well cell culture plate (8×10^5 BHK-21 cells/well). (A) Expression of EYFP was captured with fluorescence microscopy; scale bar represents 400 μm. (B) Fluorescent cell population of EYFP levels from mRNA and replicon RNA was determined by fluorescence-activated cell sorting (FACS). The graphs are plotted with side scatter area [FSC-A] versus EYFP fluorescence intensity. For statistical significance, p value was calculated using unpaired two-tailed test. * $p < 0.005$. (C) Expression of Renilla luciferase for mRNA (Luc, EYFP) and replicon forms of the reporter gene, measured from the cell lysate collected post transfection. Multifold change of

Renilla luciferase and EYFP mRNA levels for mRNA and replicon forms in transfected BHK-21 cells was determined by quantitative real-time PCR. The levels of respective mRNAs in the transfected cells were normalized by GAPDH mRNA.

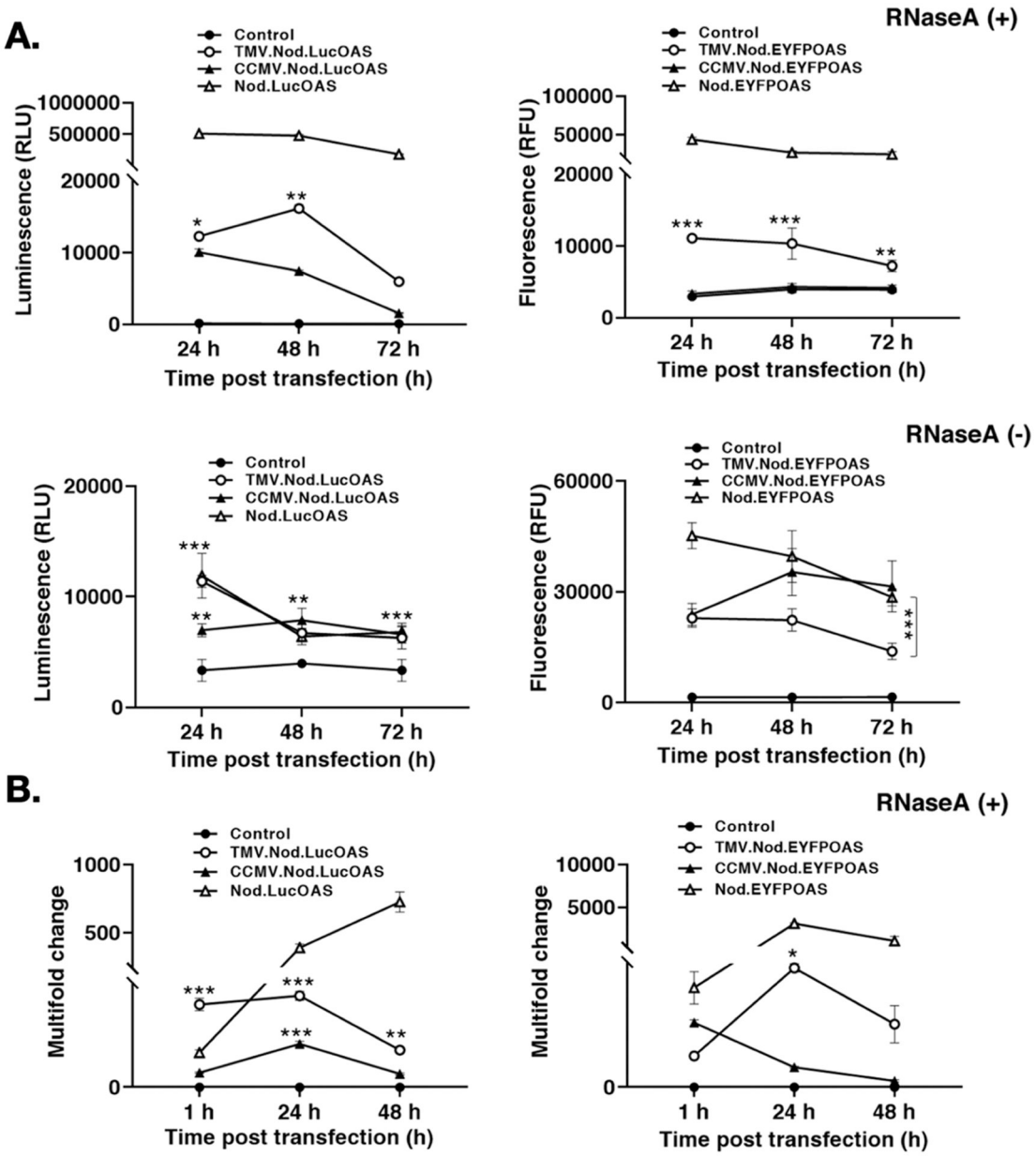

Figure 3.

In vitro delivery of reporter gene replicons in TMV and CCMV VLP-packaged forms, using lipofectamine-mediated transfection into BHK cells. (A) Expression of Renilla luciferase was measured from the cell lysates collected at different times after transfection of naked NodLuc.OAS and of RNaseA-treated (+) and *non*-RNaseA-treated (−) Nod.lucOAS-containing TMV and CCMV VLPs (750 ng of Nod.LucOAS loaded into the TMV ~ 14 μg and 1000 ng of Nod.LucOAS loaded into the CCMV ~ 3.4 μg). Expression of EYFP was measured at excitation/emission wavelengths of 500 and 540 nm from the transfected cells collected at different times after transfection of naked Nod.EYFPOAS and of RNaseA-treated (+) and *non*-RNaseA-treated (−) Nod.EYFPOAS-containing TMV and CCMV VLPs (500 ng of Nod.EYFPOAS loaded into the TMV ~ 10 μg and the CCMV ~ 1.7 μg). (B)

Multifold changes of luciferase and EYFP mRNA levels with respect to the control cells up to 48 h in the transfected BHK-21 cells were measured by quantitative real-time PCR for naked RNA and for RNase-treated TMV and CCMV VLPs. The levels of respective mRNAs in the transfected cells were normalized by the GAPDH mRNA. For statistical significance, p value was calculated by using two-way ANOVA: ***$p < 0.0001$, **$p < 0.005$, *$p < 0.05$, ns: not significant.

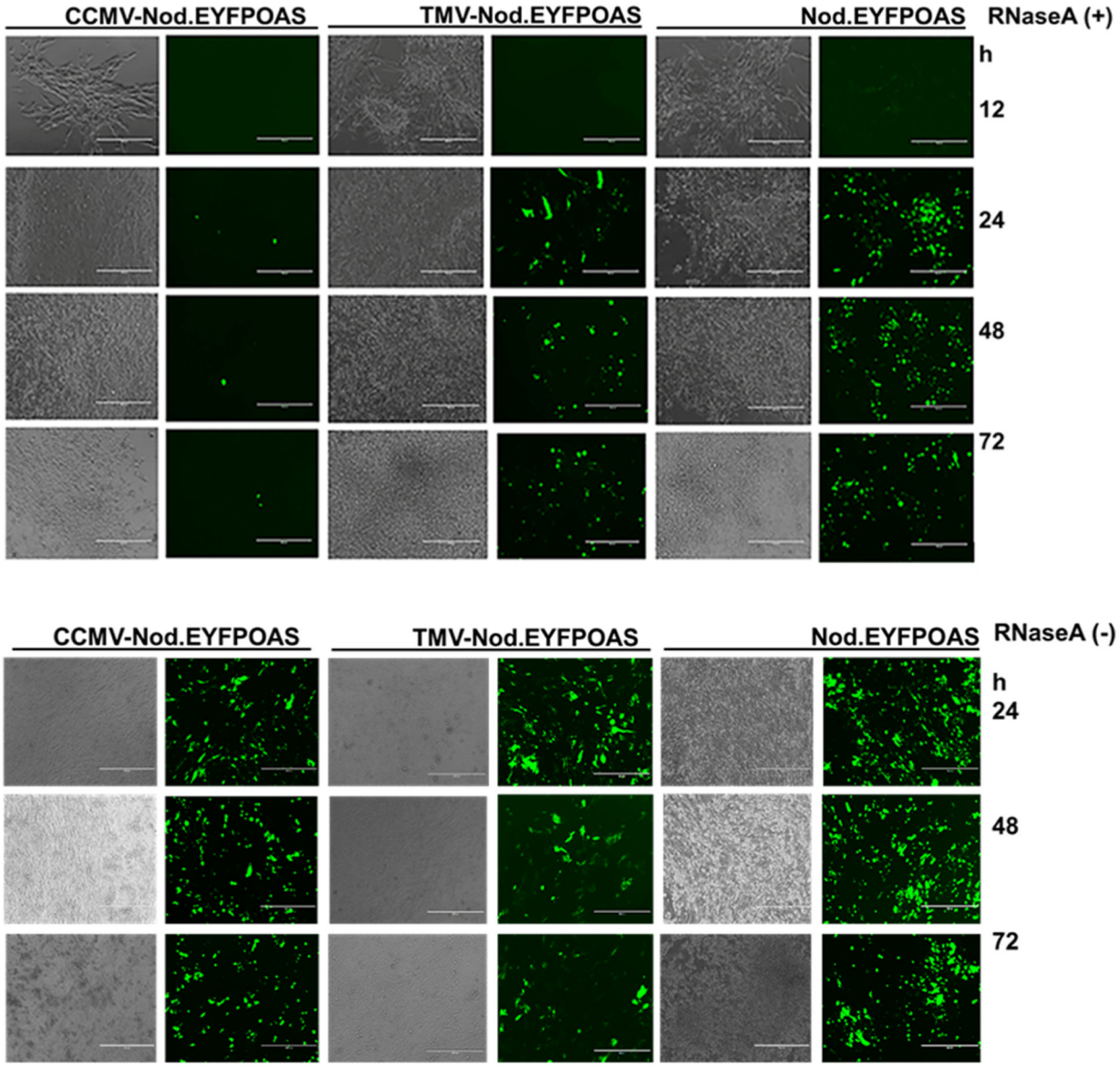

Figure 4.

Bright-field and fluorescence microscopy images of BHK cells transfected with reporter gene replicons in naked and in TMV and CCMV VLP-packaged forms. Expression of EYFP was imaged after transfection of 500 ng of the Nod.EYFPOAS replicon in naked RNA form and in RNaseA-treated (+) and non-RNaseA-treated (−) CCMV and TMV VLPs. The scale bar is 400 μm.

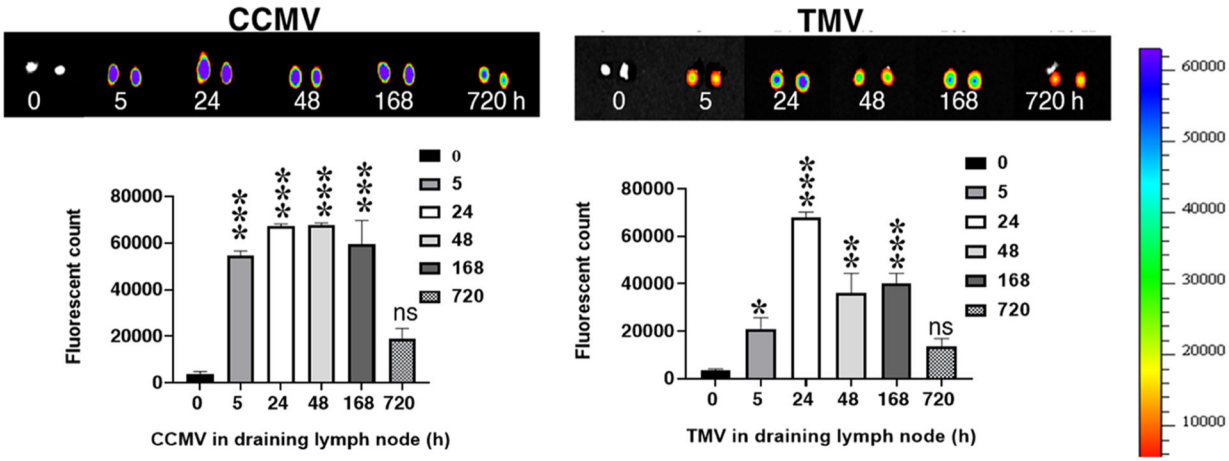

Figure 5.

In vivo delivery of genes using VLPs. (A) Lymph node trafficking and localization of VLPs in the draining lymph node. The fluorescent VLPs, Cy5.TMV and Cy5.CCMV, were delivered into the mice through footpad injection. The localization of VLPs into the draining lymph nodes was quantified from the popliteal lymph node harvested from the mice post injection from 5 to 720 h. For statistical significance, the *p* values were calculated using one-way ANOVA. ***$p < 0.0001$, **$p < 0.005$, *$p < 0.05$, ns: not significant.

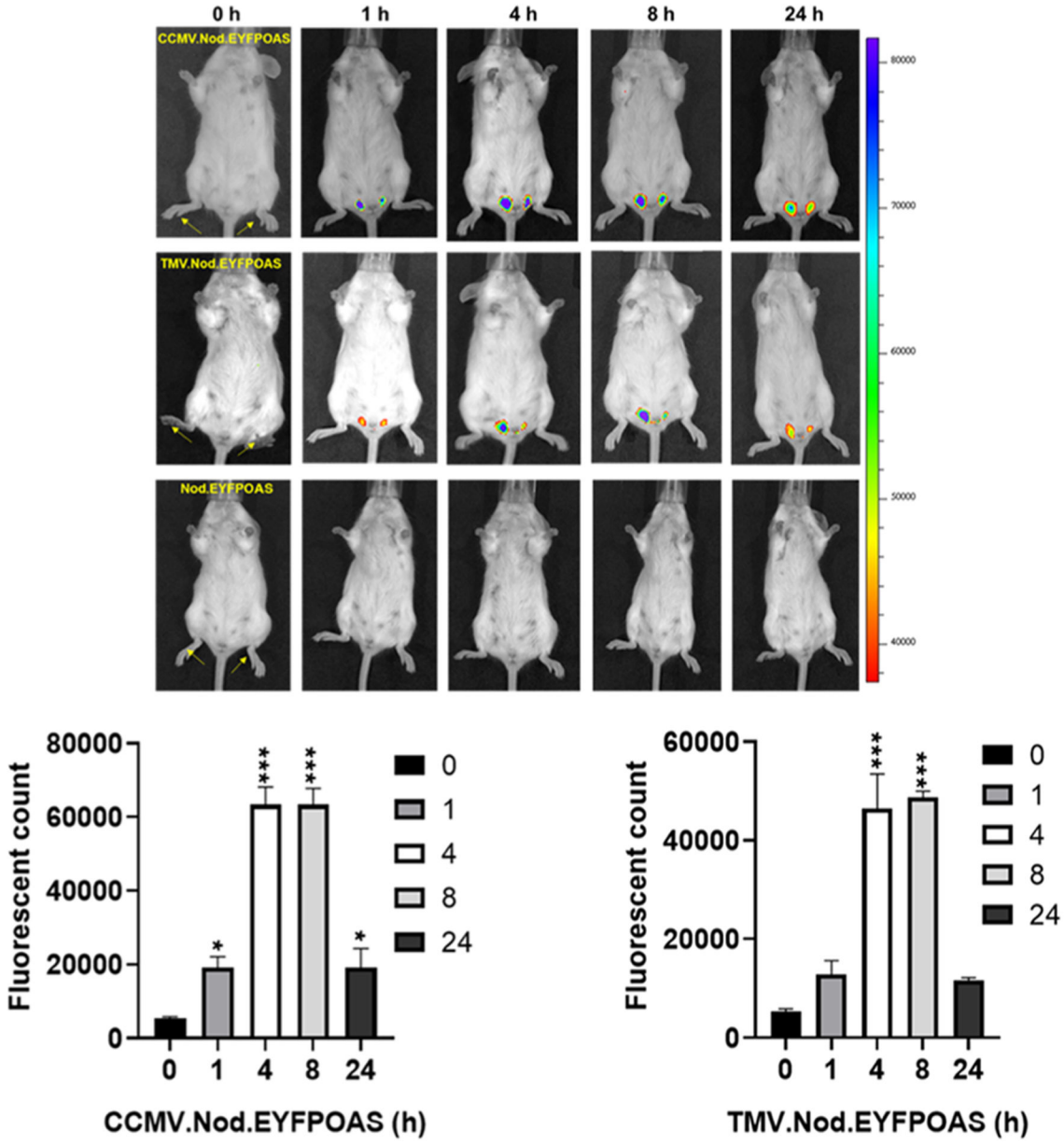

Figure 6.

In vivo delivery of genes using VLPs. *In vivo* delivery of the self-amplifying enhanced yellow fluorescent protein gene with the Nodamura replicon (5 μg mRNA) encapsulated in *non*-RNaseA-treated TMV and CCMV VLPs (100 μg) by subcutaneous injection into the footpads of mice. Upon delivery, the expression of EYFP was measured by the fluorescent signal observed in mice using IVIS spectrum optical imaging system. For statistical significance, p values were calculated using one-way ANOVA. ***$p < 0.0001$, **$p < 0.005$, *$p < 0.05$, ns: not significant.